

# A MULTIREOLUTION IMAGE RESTORATION METHOD FOR PHOTON IMAGING SYSTEMS

*Ghada Jammal*

Technische Universität Darmstadt  
Institut für Netzwerk und Signaltheorie  
Merkstraße 25, D-64283 Darmstadt  
ghada@nesi.tu-darmstadt.de

*Albert Bijaoui*

Observatoire de la Cote d'Azur  
Boîte Postale 4229  
06304 Nice Cedex 4 France  
bijaoui@obs-nice.fr

## ABSTRACT

Nuclear medicine imaging systems rely on photon detection as the basis of image formation. One of the major sources of error in these imaging systems is Poisson noise. In this paper, we develop a novel multiscale image restoration procedure for photon imaging systems. It consists in separating in the wavelet-domain data points which belong to structures from those due to the noisy background. The latter are replaced by coefficients obtained by the introduction of a multiresolution regularity constraint. The restored image represents therefore a compromise between fidelity to the data and fidelity to the a priori knowledge on the smoothness of the solution. The performance of the method is assessed with simulated data experiments.

## 1. INTRODUCTION

Nuclear medicine imaging is a widely used commercial imaging modality. As a diagnosis tool, it is unique in that it documents organ function *and* structure. It is a way to gather information that may be otherwise unavailable or require surgery. A patient undergoing a nuclear medicine exam [1] receives a very small amount of a radioactive pharmaceutical which is targeted for uptake in specific regions of the body. As the radioactive pharmaceutical decays, gamma rays are emitted from within the patient. Imaging the gamma ray emissions provides a mapping of the distribution of the pharmaceutical, and hence a mapping of the anatomy and physiologic function of the organ. The imaging system is the gamma camera which proceeds by converting gamma rays into light photons, which will be detected and located by a set of photomultiplier tubes. One of the major sources of error in these imaging systems is Poisson noise [2] which degrades such images in both qualitative and quantitative senses and hinders image analysis and interpretation. Hence, improvements in image quality represents a significant opportunity to advance the state-of-the-art in this field.

The paper is organized as follows. In section 2 we give the statistical model of the image. In section 3, we describe the structure detection in the wavelet domain and introduce the notion of significant coefficients. In section 4, we discuss the regularized reconstruction. In section 5, we derive the algorithm corresponding to the restoration method. Section 6 exposes the results of the method on simulated data experiment. Finally we outline our future work.

## 2. STATISTICAL IMAGE MODEL

The raw nuclear medicine image or scintigram is acquired by counting photon detections at different spatial locations over an observation period of  $T$  seconds. Let us define the local uptake density  $\rho(x, y, z)$  as being the number of radionuclides taken up per unit volume of the imaged organ. Let  $I(k_x, k_y)$  be the random variable „number of photon counts at position  $(k_x, k_y)$  of the scan during time  $T$ “. This variable has a Poisson distribution [3]

$$P(I(k_x, k_y) = n) = \frac{\lambda_p^n(k_x, k_y)}{n!} e^{-\lambda_p(k_x, k_y)}$$

where  $\lambda_p$  is the rate of events integrated over the counting interval  $T$ . If we suppose the desintegration constant of the radionuclide,  $\lambda_r$ , constant over time, we have:

$$\lambda_p(k_x, k_y) = \lambda_r T \int_V \rho(x, y, z) dV$$

with  $V$  being the volume of the organ corresponding to a pixel on the scan. Since  $\lambda_p(k_x, k_y)$  is not constant over the scintigram,  $I(k_x, k_y)$  obeys a non-uniform Poisson distribution. The scintigram is thus a representation of the uptake density which is corrupted by a statistical fluctuation.

## 3. STRUCTURE DETECTION

We would like to separate the data points which belongs to structures (areas of different sizes that have an abnormal uptake in comparison to the adjacent gland) from those due to the noisy background. This is performed in the wavelet domain because the wavelet transform provides a method for local analysis which has the extra advantage of yielding coefficients equal to zero for a locally constant signal [4]. Having a noisy representation of the uptake density, the wavelet coefficients associated with the scintigram could be different from zero although the underlying uptake density is constant. Consequently, the existence of structures at a given scale is tied to the presence at this scale of wavelet coefficients with a large enough absolute value [5].

### 3.1. Significant Wavelet Coefficients

In order to discern between the wavelet coefficients due to a statistical fluctuation of the counts and those due to an existing structure,

we analyse the statistical significance of the coefficients by comparison with the values obtained from a locally uniform Poissonian distribution. We are faced to a classical decision problem [6]: we focus on two hypotheses and give a rule between them based on the sample evidence. We hope to show that the uptake density varies at scale  $2^j$ , to do this we suppose for the sake of argument that the uptake density is constant at scale  $2^j$ , we then look for evidence against the supposition we made. Stating the hypotheses in terms of the wavelet coefficient of the population we have:

$$\begin{aligned} H_0 : \mathcal{W}(2^j, k_x, k_y) &= 0 \\ H_a : \mathcal{W}(2^j, k_x, k_y) &\neq 0 \end{aligned}$$

We find the probability of getting an outcome at least as far as the actually observed statistic from what we would expect when  $H_0$  is true. This probability is called the P-value and calculated as follows:

- If  $W(2^j, k_x, k_y) > 0$

$$P = \text{Prob}(\mathcal{W}(2^j, k_x, k_y) > W(2^j, k_x, k_y)) \quad (1)$$

- If  $W(2^j, k_x, k_y) < 0$

$$P = \text{Prob}(\mathcal{W}(2^j, k_x, k_y) < W(2^j, k_x, k_y)) \quad (2)$$

Where  $W(2^j, k_x, k_y)$  are the wavelet coefficients of the sample data. The evidence we obtain is then compared with the significant level  $\alpha$  which is a fixed level of evidence that we regard as decisive. If the P-value is as small or smaller than  $\alpha$ , we can not consider at the level of decision  $\alpha$  that the value of the coefficient is only due to noise. We reject  $H_0$  in favor of  $H_a$  which means that the image is not considered being constant at scale  $2^j$ . We say that we detected a statistically significant wavelet coefficient at level  $\alpha$ . If the P-value is bigger than  $\alpha$ , although non zero, we consider that the wavelet coefficient is caused by a chance fluctuation of the underlying random process and accept  $H_0$ .

### 3.2. Probability distribution of the wavelet coefficients

In order to compute the P-value, we need to compute the probability density function of the wavelet coefficient under the hypothesis  $H_0$ , that is for a locally uniform Poisson distribution. This law depends on the analysing wavelet. We will start by justifying the choice of the wavelet and then describe how we obtained the probability density function.

The 2D discrete wavelet transform is calculated using Mallat's algorithm [7] implemented as a filter bank where the application of a lowpass filter  $h$  and a highpass filter  $g$  is alternated on rows and columns of the image  $I(k_x, k_y)$ . In order to interpret the output of the filters as the wavelet series of the continuous image  $I(x, y)$ , the input signal of the filter bank,  $I(k_x, k_y)$ , must be the filtered version of  $I(x, y)$  with translated versions of the scaling function:

$$I(k_x, k_y) = \langle I(x, y), \phi(x - k_x)\phi(y - k_y) \rangle$$

In nuclear medicine imaging  $I(k_x, k_y)$  corresponds to the number of photon counts at position  $(k_x, k_y)$  of the scan; it can be interpreted as the filtered version of the continuous image  $I(x, y)$  by the scaling function which takes the value one in the surface corresponding to a pixel, and zero otherwise. This scaling function

corresponds to the Haar wavelet, which can be associated to the filters:

$$h = [1, 1] \quad g = [1, -1]$$

Let us note  $F(2^j, k_x, k_y)$  the scaling coefficient at scale  $2^j$  and  $W_h(2^j, k_x, k_y)$ ,  $W_v(2^j, k_x, k_y)$  and  $W_d(2^j, k_x, k_y)$  the horizontal, vertical and diagonal wavelet coefficients at scale  $2^j$ . The scaling and wavelet coefficients at the next scale  $2^{j+1}$  are obtained by:

$$\begin{aligned} F(2^{j+1}, k_x, k_y) &= \gamma_1 + \gamma_2 + \gamma_3 + \gamma_4 \\ W_h(2^{j+1}, k_x, k_y) &= \gamma_1 - \gamma_2 + \gamma_3 - \gamma_4 \\ W_v(2^{j+1}, k_x, k_y) &= \gamma_1 + \gamma_2 - \gamma_3 - \gamma_4 \\ W_d(2^{j+1}, k_x, k_y) &= \gamma_1 - \gamma_2 - \gamma_3 + \gamma_4 \end{aligned} \quad (3)$$

where

$$\begin{aligned} \gamma_1 &= F(2^j, k_x, k_y) & \gamma_2 &= F(2^j, k_x, k_y + 1) \\ \gamma_3 &= F(2^j, k_x + 1, k_y) & \gamma_4 &= F(2^j, k_x + 1, k_y + 1) \end{aligned}$$

Under the null hypothesis, a constant uptake density is assumed, this means that  $I(k_x, k_y) = F(2^0, k_x, k_y)$  are assumed to be Poisson variables of parameter  $\lambda_p$ . It follows that the scaling coefficients  $F(2^j, k_x, k_y)$  are Poisson variable of constant parameter  $2^{2j}\lambda_p$ . The wavelet coefficients  $W_h$ ,  $W_v$  and  $W_d$  being calculated as the difference of two sums of Poisson variables (3):  $W_{h,v,d}(2^{j+1}) = S_1 - S_2$ , where  $S_1$  and  $S_2$  are Poisson variables of parameter  $2^{2j+1}\lambda_p$ , their probability density function can be calculated as follows:

$$\begin{aligned} p(W_{h,v,d}(2^{j+1}) = \nu) &= \sum_{m=0}^{+\infty} P(S_1 = \nu + m)P(S_2 = m) \\ &= e^{-2^{2(j+1)}\lambda_p} \sum_{m=0}^{+\infty} \frac{(2^{2j+1}\lambda_p)^{\nu+2m}}{(\nu+m)!m!} \\ &= e^{-2^{2(j+1)}\lambda_p} I_\nu(2^{2(j+1)}\lambda_p) \end{aligned}$$

Where  $I_\nu(x)$  is the modified Bessel function of integer order [8].

### 3.3. Thresholding

At each scale, the significant level  $\alpha$  corresponds to a threshold that we will note  $t_{2^j}$ . The wavelet coefficients  $W$  are separated in two groups: the non significant coefficients  $X$  and the significant coefficients  $Y$  where:

$$Y(2^j, k_x, k_y) = \begin{cases} W(2^j, k_x, k_y) & \text{if } |W(2^j, k_x, k_y)| > t_{2^j}, \\ 0 & \text{otherwise.} \end{cases}$$

We thus separated the contribution of signal from that of noise.

## 4. REGULARIZED RECONSTRUCTION

Our image processing problem is to obtain an estimate  $\hat{I} = \hat{F}^i(2^0)$  of the true image  $\mathcal{I}$  using the raw data image  $I = F(2^0)$ . The solution that consists in reconstructing  $\hat{I}$  from  $Y$  taking  $X=0$  is not acceptable due to the block effects that it provoques: when a wavelet coefficient is lost by thresholding, information on the local gradient of the image is lost and the signal is reconstructed using the local mean. We therefore consider the  $X$  coefficients as unknown coefficients that have to be determined. Due to the fact

that there exists an infinity of solutions, we are faced to an ill-posed problem [9]. This problem can be resolved by introducing a priori knowledge defined by a multiresolution regularity constraint of minimum gradient [10]. The restored image takes into account the information given by the significant coefficients (fidelity to the data) but its non-significant coefficients are defined by the a priori on the smoothness of the solution (regularization constraint).

We introduce the analysis operators  $H_2$ ,  $G_h$ ,  $G_v$  and  $G_d$  so that the analysis equations of the multiresolution analysis can be written as:

$$\begin{aligned} F(2^{j+1}) &= H_2 F(2^j) & W_h(2^{j+1}) &= G_h F(2^j) \\ W_v(2^{j+1}) &= G_v F(2^j) & W_d(2^{j+1}) &= G_d F(2^j) \end{aligned}$$

and the synthesis operators  $\widetilde{H}_2$ ,  $\widetilde{G}_h$ ,  $\widetilde{G}_v$  and  $\widetilde{G}_d$  so that the synthesis equation can be written as:

$$\begin{aligned} F(2^j) &= \widetilde{H}_2 F(2^{j+1}) + \widetilde{G}_h W_h(2^{j+1}) \\ &+ \widetilde{G}_v W_v(2^{j+1}) + \widetilde{G}_d W_d(2^{j+1}) \end{aligned} \quad (4)$$

We want to find the coefficients  $W$  so that the reconstruction of the signal with these coefficients minimizes, at each scale the multiresolution gradient constraint:

$$C(2^j) = \|D_x F(2^j)\|^2 + \|D_y F(2^j)\|^2$$

where  $D_x$  and  $D_y$  are the horizontal and vertical gradient operators. The solution  $\widehat{W}_h(2^{j+1})$ ,  $\widehat{W}_v(2^{j+1})$  and  $\widehat{W}_d(2^{j+1})$  must minimize  $C(2^j)$ . This leads to

$$\begin{aligned} \frac{\partial C(2^j)}{\partial \widehat{W}_h(2^{j+1})} &= G_h L_2 F(2^j) = 0 \\ \frac{\partial C(2^j)}{\partial \widehat{W}_v(2^{j+1})} &= G_v L_2 F(2^j) = 0 \\ \frac{\partial C(2^j)}{\partial \widehat{W}_d(2^{j+1})} &= G_d L_2 F(2^j) = 0 \end{aligned}$$

Replacing  $F(2^j)$  by (4), we obtain a system of the form  $\mathcal{Y} = \mathcal{A}\mathcal{X}$  where the vector  $\mathcal{Y}$  is known,  $\mathcal{A}$  is the operator to inverse and  $\mathcal{X}$  is the unknown vector. In order to make the inversion, we use the Van-Cittert algorithm [11] which leads to an iterative solution of the form:

$$\begin{aligned} \widehat{W}_h^{(n+1)}(2^{j+1}) &= \widehat{W}_h^{(n)}(2^{j+1}) - \alpha G_h L_2 \widehat{F}^{(n)}(2^j) \\ \widehat{W}_v^{(n+1)}(2^{j+1}) &= \widehat{W}_v^{(n)}(2^{j+1}) - \alpha G_v L_2 \widehat{F}^{(n)}(2^j) \\ \widehat{W}_d^{(n+1)}(2^{j+1}) &= \widehat{W}_d^{(n)}(2^{j+1}) - \alpha G_d L_2 \widehat{F}^{(n)}(2^j) \end{aligned} \quad (5)$$

where  $L_2$  corresponds to the laplacian obtained by convolution with the filter:

$$\begin{bmatrix} 0 & -1 & 0 \\ -1 & 4 & -1 \\ 0 & -1 & 0 \end{bmatrix}$$

## 5. ALGORITHM

We apply a coarse to fine processing to the wavelet coefficients of the raw data image  $I = F(2^0)$ : the restoration starts with the lowest resolution  $2^{j_m}$  until it reaches the resolution  $2^0$ . The Poisson parameter is first supposed to be constant over the whole image and taken as the original image mean, it is then progressively modified and takes the value  $\lambda_p^i(k_x, k_y) = \widehat{F}^i(2^0)$ . This leads to the following algorithm:

1. Compute the wavelet coefficients  $W_h, W_v, W_d$  of the raw data image  $I$  until the desired resolution  $2^{j_m}$  is reached.
  2. Initialize  $i$  to 0 and start with the constant Poisson parameter  $\lambda_p^i = \sum I / \text{number of pixels of } I$ . Let  $\epsilon_0$  be a convergence parameter.
  3. Start at the lowest resolution  $2^j = 2^{j_m}$  and initialize  $n$  to 0, let  $\epsilon_1$  be a convergence parameter.
  4. Compute  $F^{(n)}(2^{j-1})$  using (4).
  5. Compute the residuals
    - $R_h^{(n)}(2^j) = G_h L_2 F^{(n)}(2^{j-1})$
    - $R_v^{(n)}(2^j) = G_v L_2 F^{(n)}(2^{j-1})$
    - $R_d^{(n)}(2^j) = G_d L_2 F^{(n)}(2^{j-1})$
  6. Compute the new solution using (5). Only the non-significant wavelet coefficients  $\hat{X}$  must be modified. The significant coefficients remain unchanged.
  7. Convergence test:
    - if  $\|R^{(n)}(2^j, k_x, k_y) - R^{(n-1)}(2^j, k_x, k_y)\|^2 < \epsilon_1$  for each of the 3 wavelets planes, go to step 8.
    - else  $n \leftarrow n + 1$ , go to step 4.
  8. if  $j=0$  then
    - if  $\|\widehat{F}^i(2^0) - \widehat{F}^{i-1}(2^0)\|^2 < \epsilon_0$ , end of the algorithm. The reconstructed image is  $\hat{I} = \widehat{F}^i(2^0)$ .
    - else  $i \leftarrow i + 1$ ,  $\lambda_p^i(k_x, k_y) = \widehat{F}^i(2^0)$  go to step 3.
- else  $j \leftarrow j - 1$ ,  $n = 0$ , go to step 4 to restore the next resolution .

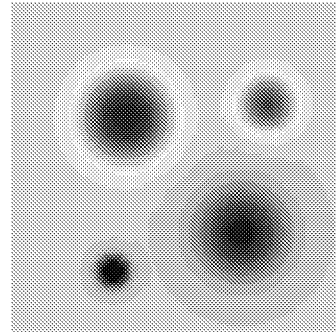


Figure 1: True image  $\mathcal{I}$

## 6. SIMULATED DATA EXPERIMENT

Nuclear medicine imaging is of particular importance in the detection of the nodular thyroid disease that is the development by the thyroid of one or more localized swellings called nodules. Thyroid nodules do not function like normal thyroid tissue. They take up less (cold nodule) or more (hot nodule) radioactive material than the normal thyroid tissue and may be cancerous. The major challenge facing a physician examining a thyroid scan is to identify the nodules and to classify them as hot or cold.

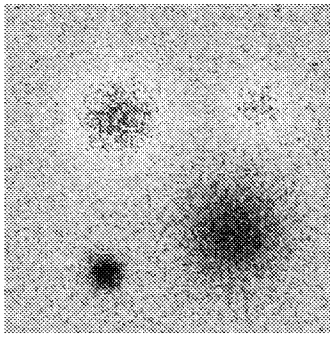


Figure 2: Raw image  $I$

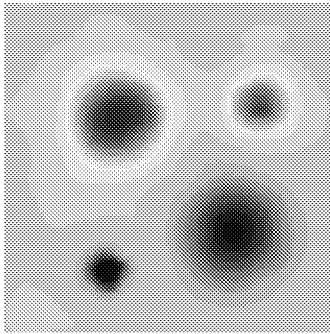


Figure 3: Reconstructed image  $\hat{I}$

In this section we present a simulated imaging experiment in order to assess the performance of our restoration method on scintigrams of the thyroid. The simulated intensity image  $\mathcal{I}$  (fig. 1) consists of a background of constant intensity where nodules are represented by a gaussian intensity profile. It was designed to have an intensity range similar to that encountered in nuclear medicine imaging. The nodules exhibit different contrasts with respect to the local environment and are of different sizes. Fig. 2 shows the raw count image  $I$  obtained from the intensity image by the introduction of Poisson noise. The reconstructed image  $\hat{I}$  is shown in fig. 3. The algorithm did a good job of reducing the background noise:  $\text{mse}(I, \mathcal{I}) = 49.5$ ;  $\text{mse}(\hat{I}, \mathcal{I}) = 0.9$ . Qualitatively, the objects in the image have been protected in the sense that intensity-related, position-related, and morphological information remained faithful to the original data. Moreover, the method leads to a compression of the signal: the sole knowledge of the significant coefficients permits under the use of the regularization constraint to obtain the reconstructed image. It therefore suffices to store the significant coefficients instead of storing the raw image. This results in an important gain of storage place (we reached in our example a storage gain of 210:1).

## 7. FUTURE WORK

We are currently investigating the intensity and size sensibility of the method (minimum size and/or intensity that a structure must have to be recognized as such). Intensity-related and position-related measures will be introduced to measure quantitatively the accuracy of the restoration. The performances will then be tested

with nuclear medicine imagery. Future work will introduce the point spread function of the imaging system.

Finally we mention that this restoration method is applicable to all applications where photon detection lies at the heart of the image formation process including astronomical and low-light imaging.

## 8. REFERENCES

- [1] J.A. Sorenson and M.E. Phelps. *Physics in nuclear medicine*. New York: Grune and Stratton, 1980.
- [2] H.H. Barrett. Objective assessment of image quality: effects of quantum noise and object variability. *J. Opt. Soc. Am. A*, 7(7):1266–1278, July 1990.
- [3] B. Saleh. *Photoelectrons statistics*. Springer Verlag, 1978.
- [4] I. Daubechies. *Ten lectures on wavelets*. SIAM, Philadelphia, Pennsylvania, 1992.
- [5] J.L. Starck, F. Murtagh, and A. Bijaoui. Multiresolution support applied to image filtering and restoration. *Graphical models and image processing*, 57(5):420–431, 1995.
- [6] A.S. Moore. *Statistics concepts and controversies*. W.H. Freeman and Company New York, 1991.
- [7] S. Mallat. A theory for multiresolution signal decomposition: the wavelet representation. *IEEE Trans. on pattern analysis and machine intelligence*, 11(7):674–693, July 1989.
- [8] A. Gray and G.B. Mathews. *A treatise on Bessel functions and their applications to physics*. Macmillan and co. London, 1952.
- [9] G. Demoment. Image reconstruction and restoration: overview of common estimation structures and problems. *IEEE transactions on acoustics, speech and signal processing*, 37(12):2024–2036, Dec 1989.
- [10] Y. Bobichon and A. Bijaoui. A regularized image restoration algorithm for lossy compression in astronomy. *Experimental astronomy*, 7(3):239–255, 1997.
- [11] P.H. Van Cittert. *Zeitschrift f. Physik*, 69:298, 1931.